Article

Enhanced in vitro osteoblast differentiation on TiO_2 scaffold coated with alginate hydrogel containing simvastatin

Journal of Tissue Engineering
4: 2041731413515670
© The Author(s) 2013
Reprints and permissions:
sagepub.co.uk/journalsPermissions.nav
DOI: 10.1177/2041731413515670
tejaut.sagepub.com
SAGE

Helen Pullisaar[1], Hanna Tiainen[1], Maria A Landin[2], Ståle P Lyngstadaas[1], Håvard J Haugen[1], Janne E Reseland[1] and Esben Østrup[1,3]

Abstract

The aim of this study was to develop a three-dimensional porous bone graft material as vehicle for simvastatin delivery and to investigate its effect on primary human osteoblasts from three donors. Highly porous titanium dioxide (TiO_2) scaffolds were submerged into simvastatin containing alginate solution. Microstructure of scaffolds, visualized by scanning electron microscopy and micro-computed tomography, revealed an evenly distributed alginate layer covering the surface of TiO_2 scaffold struts. Progressive and sustained simvastatin release was observed for up to 19 days. No cytotoxic effects on osteoblasts were observed by scaffolds with simvastatin when compared to scaffolds without simvastatin. Expression of osteoblast markers (collagen type I alpha 1, alkaline phosphatase, bone morphogenetic protein 2, osteoprotegerin, vascular endothelial growth factor A and osteocalcin) was quantified using real-time reverse transcriptase–polymerase chain reaction. Secretion of osteoprotegerin, vascular endothelial growth factor A and osteocalcin was analysed by multiplex immunoassay (Luminex). The relative expression and secretion of osteocalcin was significantly increased by cells cultured on scaffolds with 10 µM simvastatin when compared to scaffolds without simvastatin after 21 days. In addition, secretion of vascular endothelial growth factor A was significantly enhanced from cells cultured on scaffolds with both 10 nM and 10 µM simvastatin when compared to scaffolds without simvastatin at day 21. In conclusion, the results indicate that simvastatin-coated TiO_2 scaffolds can support a sustained release of simvastatin and induce osteoblast differentiation. The combination of the physical properties of TiO_2 scaffolds with the osteogenic effect of simvastatin may represent a new strategy for bone regeneration in defects where immediate load is wanted or unavailable.

Keywords

Simvastatin, TiO_2 scaffold, alginate hydrogel, osteocalcin, bone morphogenetic protein 2, vascular endothelial growth factor A

Received: 24 September 2013; accepted: 14 November 2013

Introduction

The use of autologous bone graft is currently the gold standard in reconstructive bone surgery,[1] despite its many disadvantages for the patient, such as increased risk of donor site infections, fractures, nerve injuries, chronic pain, hernias and haematoma.[2] A promising alternative to autografts has however emerged with the idea of using synthetic three-dimensional (3D) bone graft substitutes with a delivery system for bioactive agents. Compounds such as bone morphogenetic proteins,[3] growth factors[4] and pharmaceutical compounds[5,6] have all been incorporated into bone-specific drug delivery systems with the primary goal of supporting new bone formation at the site of a defect.[7]

[1]Department of Biomaterials, Institute of Clinical Dentistry, University of Oslo, Oslo, Norway
[2]Oral Research Laboratory, Institute of Clinical Dentistry, University of Oslo, Oslo, Norway
[3]Norwegian Center for Stem Cell Research, Institute of Immunology, Oslo University Hospital, Rikshospitalet, University of Oslo, Oslo, Norway

Corresponding Author:
Håvard J Haugen, Department of Biomaterials, Institute of Clinical Dentistry, University of Oslo, Geitmyrsveien 71, P.O. Box 1109, Blindern, NO-0317 Oslo, Norway.
Email: h.j.haugen@odont.uio.no

In recent years, there has been an increase in the interest towards simvastatin (SIM) and its effect on bone.[8–11] SIM is a member of the statin family of 3-hydroxy-3-methylglutaryl coenzyme A reductase inhibitors. This cholesterol-lowering drug is known to elicit numerous pleiotropic effects[12] including enhancement of bone formation through anabolic[13] and anti-catabolic mechanisms.[14] Several drug delivery systems such as hydrogels,[15] collagen sponges[16] or modified implant surfaces[17,18] have been described for use in bone tissue engineering. However, only a few studies have focused on drug delivery systems suitable for reconstructive bone surgery.[19–21] Such a system should not only provide long-term drug release kinetics but also mechanical support and a porous structure to allow ingrowth of new bone.[22,23] No reports have so far been made on porous SIM delivery systems for load-bearing bone tissue applications with primary human osteoblasts.

Previously, the development of porous and well-interconnected titanium dioxide (TiO_2) scaffold with high mechanical strength has been described.[24] Biocompatibility and osteoconductive properties of the TiO_2 scaffold have been demonstrated in vitro[25–27] and in vivo.[28,29] The aim of the present study was to develop a 3D porous SIM delivery system for use in load-bearing bone and to examine its effect on primary human osteoblasts from three donors.

Materials and methods

Fabrication of TiO_2 scaffolds coated with alginate hydrogel containing SIM

Porous TiO_2 scaffolds, 8 mm in height and a diameter of 9 mm, were produced by polymer sponge replication as previously described.[30] In short, polymer foams were impregnated with TiO_2 slurry, dried and subsequently sintered at 1500°C for 40 h. A second layer of TiO_2 slurry was added to the scaffolds and re-sintered at the same temperature as previously mentioned. Total surface area of the scaffolds, determined by micro-computed tomography (micro-CT) (SkyScan 1172; Kontich, Belgium), was 20.295 cm^2. Produced scaffolds were sterilized by autoclaving at 121°C for 20 min.

SIM (Krebs Biochemicals & Industries, Andhra Pradesh, India) was dissolved in 100% ethanol to 10 mM before being added to 2% (w/v) Pronova UP LVG sodium alginate (FMC BioPolymer, Sandvika, Norway) in milliQ water at desired concentrations to create SIM-containing alginate-coated TiO_2 scaffolds. Alginate solution with or without SIM was sterilized before use with a 0.22-μm pore size syringe filter (TPP Techno Plastic Products AG, Trasadingen, Switzerland).

The alginate-coated scaffolds with SIM were submerged into alginate solution with SIM (2.4 mM, 0.6 mM, 24 μM, 10 μM, 1 μM, 0.1 μM and 10 nM) under agitation at 100 r/min on an orbital shaker for 1 h at room temperature followed by centrifugation at 300 × g for 1 min to remove the excess alginate solution. Subsequently, scaffolds were immersed into 50 mM $CaCl_2$ with SIM (2.4 mM, 0.6 mM, 24 μM, 10 μM, 1 μM, 0.1 μM and 10 nM) under agitation at 100 r/min on an orbital shaker for 1 h. SIM was added to the $CaCl_2$ solution to inhibit its diffusion out from the alginate coating during the gelling procedure. Alginate-coated scaffolds were finally rinsed with milliQ water to remove the excess $CaCl_2$ and air-dried overnight. The scaffolds in the control group, alginate-coated scaffolds without SIM, were treated in the same way as the alginate-coated scaffolds with SIM, except that alginate and $CaCl_2$ solutions did not contain SIM.

Characterization of TiO_2 scaffolds coated with alginate hydrogel containing SIM

The alginate-coated scaffolds were gold-sputtered (Cressington sputter coater 108 auto, Cressington Scientific Instruments, Watford, England) and their microstructure was visualized by scanning electron microscopy (SEM) (TM-1000; Hitachi High-Technologies, Tokyo, Japan) with backscattered secondary ions at 15 kV accelerating voltage. Alginate coating was further assessed by micro-CT. In brief, the dried alginate-coated TiO_2 scaffolds (N = 5) were immersed into Omnipaque iohexol radiographic contrast agent (GE Healthcare, Oslo, Norway) in milliQ water at 150 mg/mL concentration for overnight, followed by centrifugation at 300 × g for 1 min to remove the contrast medium. Then, the scaffolds were mounted vertically on a plastic sample holder and scanned with micro-CT imaging system at 4.5 μm voxel resolution using source voltage of 100 kV and current of 100 μA with 0.5-mm aluminium filter. The scaffolds were rotated 180° around their vertical axis, and three absorption images were recorded every 0.3° of rotation. The raw images were reconstructed with the standard SkyScan reconstruction software (NRecon) to a 3D cross-sectional image dataset using a 3D cone beam reconstruction algorithm. For the reconstruction, beam hardening was set to 0%, smoothing 0 and ring artefact reduction to 20. The image analysis of the reconstructed images was performed using the standard SkyScan software (CTan and CTvol). The scaffold morphology was analysed in two cylindrical volumes of interest with a diameter of 4.5 mm and a height of 4.5 mm in the centre and at the edge of the scaffolds. The pore architecture was characterized by determining the porosity, pore size and interconnectivity as previously described.[24]

Quantification of SIM release from alginate-coated TiO_2 scaffolds

Alginate-coated scaffolds and SIM-containing (2.4 mM, 0.6 mM) alginate-coated scaffolds were kept at 37°C in 1 mL milliQ water in a humidified atmosphere for up to 19 days

to determine the release profile of SIM. At prefixed time points (0.25 days, 2 days, 4 days, 6 days, 8 days, 10 days, 13 days, 15 days, 17 days, 19 days), the milliQ water was replaced, and the amount of SIM released was quantified using ultraviolet–visible (UV-Vis) spectrophotometer (PerkinElmer Lambda 25 UV/Vis System; PerkinElmer, Waltham, MA, USA). The sample absorbance at a wavelength of 238 nm was analysed and the relative absorbance units were correlated with the amount of SIM released for each time point using a linear standard curve. Absorbance values from scaffolds coated with alginate without SIM were used as control to subtract background values obtained from alginate degradation products. The experiment was performed in triplicate.

Cell culture and seeding of primary human osteoblasts

Primary human osteoblasts (hOBs) (Cambrex Bio Science, Walkersville, MD, USA) from three donors, two from femur (16- and 10-year-old males) and one from tibia (41-year-old male) were cultured in osteoblast culture medium supplemented with 10% fetal bovine serum, 0.1% gentamicin sulphate, amphotericin-B and ascorbic acid (Lonza, Walkersville, MD, USA) in 75-cm^2 culture flasks at 37°C in a humidified atmosphere of 5% CO_2. At the time of cell seeding, the hOBs from tibia had reached passage 9 and the hOBs from the two femur donors had reached passages 7 and 8, respectively. Scaffolds presoaked with culture medium were placed in 48-well culture plates, and the cell suspension was added drop-wise on the top of the scaffolds at a density of 4×10^5 cells/scaffold in 1 mL of culture medium. In order to ensure a homogenous cell distribution throughout the scaffold, an agitated seeding method was used.[31] After seeding, the plates were agitated on an orbital shaker at 200 r/min for 6 h at 37°C in humidity conditions. Cell-seeded scaffolds were transferred to new culture plates in 1 mL culture medium and maintained at 37°C in a humidified atmosphere of 5% CO_2 for up to 21 days. Triplicates of each donor, each treatment and for three harvest time points were included, in total 81 scaffolds. The culture medium was replaced every other day and collected for analyses. Scaffolds were harvested after 7, 14 and 21 days of culture for use in real-time reverse transcriptase–polymerase chain reaction (RT-PCR) and immunocytochemistry.

Cytotoxicity assay

The cytotoxicity of the SIM-containing scaffolds was estimated based on the activity of the cytostolic enzyme lactate dehydrogenase (LDH) in the culture medium. The LDH activity was determined in the medium collected every other day up till 14 days, according to the manufacturer's cytotoxicity detection kit instructions (Roche Diagnostics, Mannheim, Germany). A total of 50 μL of sample was incubated with 50 μL of the kit reaction mixture for 30 min in the dark at room temperature. The absorbance of the samples was measured at 492 nm in a plate reader (Biochrom Asys Expert 96 Microplate Reader; Biochrom, Holliston, MA, USA).

Alkaline phosphatase activity assay

The ability of alkaline phosphatase (ALP) to hydrolyse *p*-nitrophenyl phosphate (pNPP) substrates (Sigma–Aldrich, St. Louis, MO, USA) into the yellow end-product, *p*-nitrophenol was used to quantify the ALP activity in the medium after 2, 8, 14 and 21 days of culture. A quantity of 25 μL of sample was incubated with 100 μL pNPP for 30 min in the dark at room temperature and subsequently 50 μL of 3 M NaOH was added to stop the reaction. The absorbance was measured at 405 nm in a plate reader and the ALP activity was quantified using a standard curve based on calf intestinal ALP (Promega, Madison, WI, USA).

Immunoassay: quantification of secreted proteins

Aliquots of the collected culture medium were up-concentrated 8-fold using a modified PES 3K centrifugal filter (VWR, Radnor, PA, USA) according to the manufacturer's instructions. Multianalyte profiling of protein levels in the concentrated cell culture medium was performed on the Luminex 200 system (Luminex, Austin, TX, USA) using xMAP technology. Acquired fluorescence data were analysed by the xPONENT 3.1 software (Luminex). The amount of osteoprotegerin (OPG), osteocalcin (OC) and vascular endothelial growth factor A (VEGFA) in the culture medium was measured using the human bone panel and human cytokine/chemokine kits (Millipore, Billerica, MA, USA) after 2, 8, 14 and 21 days of culture. All analyses were performed according to the manufacturer's protocols.

RNA isolation and real-time RT-PCR analysis

Total RNA was isolated from cell-seeded scaffolds using the Qiagen RNA mini-kit (Qiagen, Hilden, Germany) with slight modifications to the manufacturer's protocol. Briefly, scaffolds were immersed into lysis buffer for 1 h at 4°C followed by agitation on an orbital shaker at 300 r/min for 10 min at room temperature. Subsequently, the scaffolds were discarded and the lysate buffer was sonicated (Sonics Vibra-Cell VC130PB, Newtown, CT, USA) at 2 W for 30 s. The remaining procedures followed the protocol provided by the manufacturer.

The complementary DNA (cDNA) was synthesized with RevertAid First Strand cDNA Synthesis Kit (Fermentas, St Leon-Rot, Germany) using oligo dT primers. Real-time PCR

Table 1. Primer sequences used for real-time RT-PCR assays.

Gene	Sequence of left primer	Sequence of right primer
GAPDH	CTCTGCTCCTCCTGTTCGAC	ACGACCAAATCCGTTGACTC
COL1A1	CATCTCCCCTTCGTTTTTGA	CCAAATCCGATGTTTCTGCT
ALPL	GACAAGAAGCCCTTCACTGC	AGACTGCGCCTGGTAGTTGT
BMP2	TCAAGCCAAACACAAACAGC	AGCCACAATCCAGTCATTCC
TNFRSF11B	TGGGAGCAGAAGACATTGAA	GTGTCTTGGTCGCCATTTTT
VEGFA	TCTTCAAGCCATCCTGTGTG	ATCTGCATGGTGATGTTGGA
BGLAP	GCAAGTAGCGCCAATCTAGG	GCTTCACCCTCGAAATGGTA

RT-PCR: reverse transcriptase–polymerase chain reaction; *GAPDH*: glyceraldehyde-3-phosphate dehydrogenase; *COL1A1: collagen type I alpha 1; ALPL: alkaline phosphatase; BMP2: bone morphogenetic protein 2; TNFRSF11B: osteoprotegerin; VEGFA: vascular endothelial growth factor A; BGLAP: osteocalcin.*

was performed in the ViiA™ 7 Real-Time System (Life Technologies, Paisley, UK) using SsoAdvanced™ SYBR® Green Supermix. Three-step amplification (40 cycles: 5 s 95°C, 60 s 60°C, 30 s 72°C) was implemented. No amplification control and no template control were used. Real-time RT-PCR was done for glyceraldehyde-3-phosphate dehydrogenase (*GAPDH*), collagen type I alpha 1 (*COL1A1*), ALP (*ALPL*), bone morphogenetic protein 2 (*BMP2*), OPG (*TNFRSF11B*), *VEGFA* and OC (*BGLAP*). The primer sequences are listed in Table 1. Real-time RT-PCR data were analysed using the efficiency corrected ΔΔCT method.[32]

Calcium analysis

Calcium content in the cell culture medium was determined by atomic absorption spectroscopy (AAS) (Analyst 400, PerkinElmer, Norwalk, CT, USA) after 4, 10, 16 and 20 days of culture. Samples and standards were prepared according to PerkinElmer's analytical methods for AAS. Prior to analysis, lanthanum chloride (VWR, Fontenay-sous-Bois, France) was added to the samples and standards to a final concentration of 0.5% (w/v) in order to counteract the negative effect of phosphorus on calcium sensitivity of the spectrophotometer. The absorbance was measured at 422.7 nm using an air–acetylene flame. Calcium content was calculated by WinLab32 AA Flame software (PerkinElmer) using a standard curve based on calcium carbonate (Sigma–Aldrich, St. Louis, MO, USA).

Immunocytochemistry and confocal laser scanning microscopy

After 21 days of culture, scaffolds were cut in half by a scalpel and fixed in 4% paraformaldehyde (PFA)/4.6% D-Mannitol for 15 min and subsequently stored in 1% PFA/4.6% D-Mannitol until further processing. Fixed scaffolds were submitted to heat-induced epitope retrieval by heating to 95°C in 0.05% citraconic anhydride in milliQ water (pH 7.4) for 15 min, incubated with monoclonal mouse anti-human collagen type I antibody (I-8H5, MP Biomedicals, Santa Ana, CA, USA) diluted to 1 µg/mL in 1.25% bovine serum albumin (BSA) in phosphate-buffered saline (PBS) with 0.2% Triton X for 1 h at room temperature, followed by incubation for 30 min at room temperature in Cy3-conjugated donkey anti-mouse IgG (Jackson ImmunoResearch, West Grove, PA, USA) diluted in 2.5% BSA/0.05% Tween-20/PBS at a concentration of 2 mg/mL. Cell-seeded whole mount stained scaffolds were counterstained using 4′,6-diamidino-2-phenylindole (DAPI), placed on a coverslip and covered with Dako fluorescent mounting medium (Dako, Glostrup, Denmark). Confocal laser scanning microscopy was performed on a FluoView 1000 confocal laser scanning microscope (CLSM) (Olympus, Center Valley, PA, USA). The scaffold surfaces were visualized using the CLSM in reflection mode. Images were analysed using ImageJ (NIH, Bethesda, MD, USA).

Statistics

The data obtained by cytotoxicity, ALP activity, gene expression, protein and calcium secretion analyses were compared between the groups using Holm-Sidak test following a parametric one-way analysis of variance (ANOVA). Where the equal variance and/or the normality test failed, a Kruskal–Wallis one-way ANOVA on ranks was performed (SigmaPlot 12.3, Systat Software, San Jose, CA, USA). A probability of ≤0.05 was considered significant.

Results

Characterization of TiO_2 scaffolds coated with 2% alginate hydrogel

SEM analysis of the alginate-coated scaffolds indicated that the immersion-centrifugation technique resulted in an even distribution of the alginate, coating the surface of the TiO_2 scaffold struts (Figure 1(a)–(c)). Only minor variations were seen in the distribution of the alginate, as visualized by micro-CT on the top of (Figure 2(a)) and in the middle of (Figure 2(b)) the TiO_2 scaffold. The alginate-coated scaffolds maintained highly porous well-interconnected pore structure (Table 2).

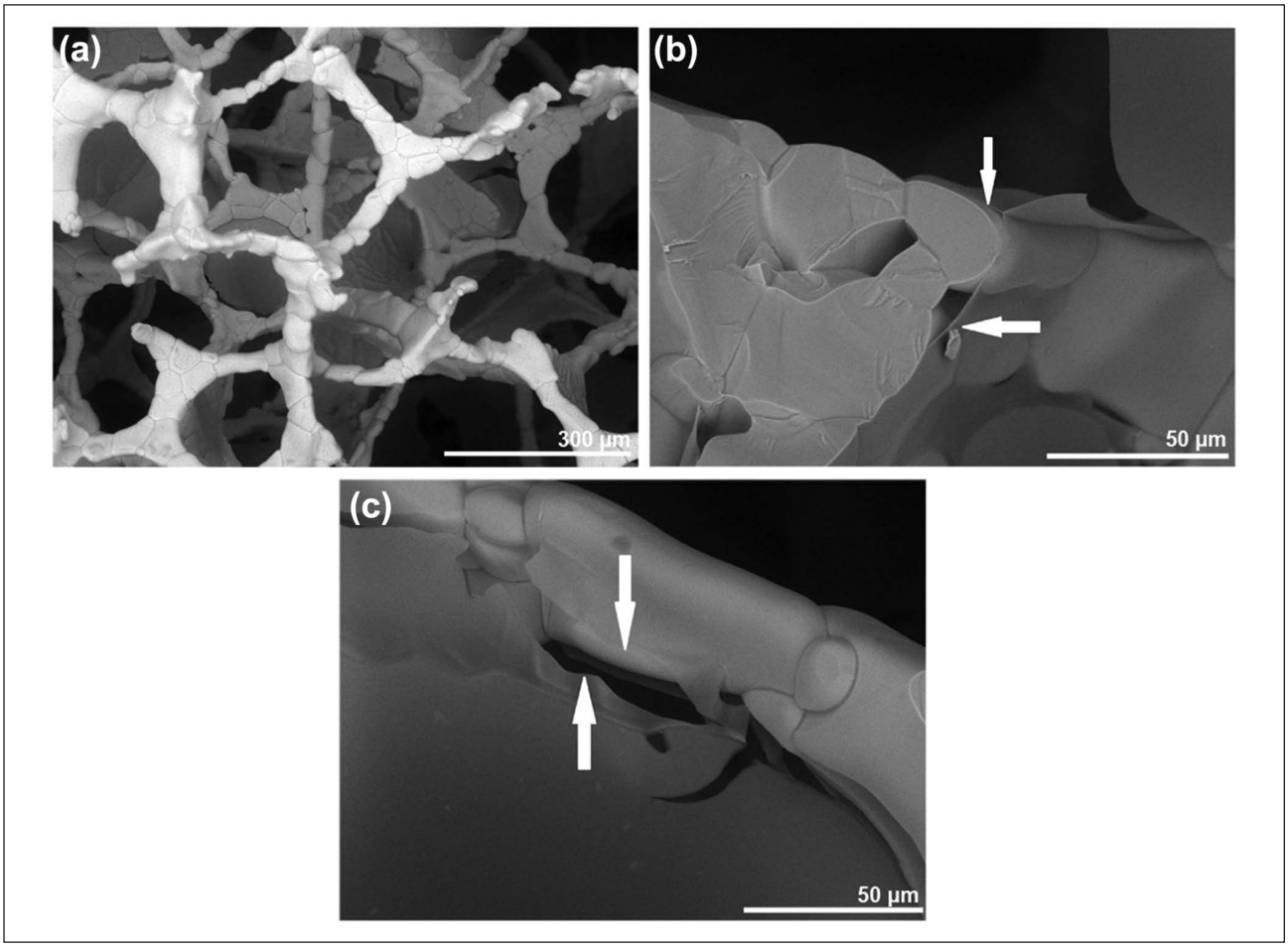

Figure 1. Scanning electron microscope characterization of alginate-coated TiO_2 scaffolds. Scanning electron microscope visualization of alginate layer (arrows) coating the strut surface of TiO_2 scaffolds at (a) 250× and (b, c) 1500× of magnification.

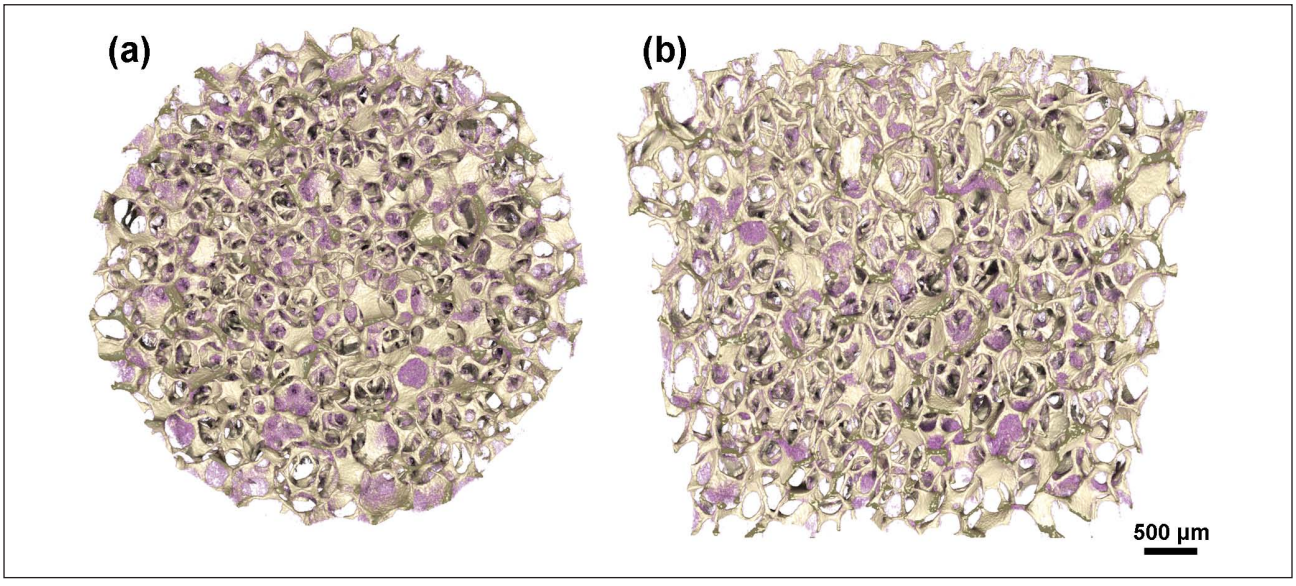

Figure 2. 3D micro-computed tomography models of alginate-coated TiO_2 scaffolds. The alginate (purple) is distributed throughout the scaffold as seen in the view from the (a) top and in the (b) middle without compromising the desired pore architectural characteristics of the TiO_2 scaffold.
3D: three-dimensional.

Table 2. Selected pore architectural features of alginate-coated and uncoated TiO_2 scaffolds.

Parameter	Unit	Alginate-coated TiO_2 scaffold	Uncoated TiO_2 scaffold
Porosity	%	88.2 ± 1.1	95.0 ± 0.7
Pore size	μm	387.2 ± 31.0	465.0 ± 25.9
Interconnectivity[a] < 100 μm	%	72.2 ± 3.8	94.5 ± 0.8

SD: standard deviation.
Values represent the mean ± SD.
[a]Interconnectivity through connections smaller than 100 μm.

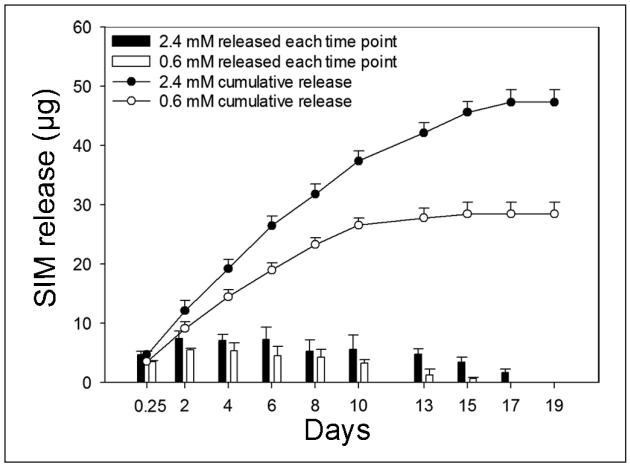

Figure 3. Simvastatin (SIM) release. Release profile of SIM from alginate-coated TiO_2 scaffolds containing 2.4 mM and 0.6 mM SIM after 19-day incubation at 37°C. Bar graph shows the amount of SIM released after each time point. Line graph represents cumulative amount of SIM released up to 19 days. Values represent the mean ± SD.
SD: standard deviation.

SIM release

The release of SIM was investigated for scaffolds with 2.4 mM and 0.6 mM SIM. A slow sustained release of SIM was detected for both concentrations. However, scaffolds with 2.4 mM SIM resulted, in a longer, 17-day release period compared to the 15-day release seen for scaffolds with 0.6 mM SIM (Figure 3). The cumulative release suggested that SIM remained entrapped in the alginate even after 19 days of incubation. Continued release could not be detected as the concentration after this point was below the detection limit.

LDH activity

The cytotoxic effect of SIM from alginate-coated scaffolds was tested for a wide range of concentrations (2.4 mM, 0.6 mM, 24 μM, 10 μM, 1 μM, 0.1 μM and 10 nM). SIM was found to be highly cytotoxic for osteoblasts at higher concentrations (above 10 μM), when cells were seeded on the scaffolds (data not shown). A 14-day cytotoxicity study was performed for lower concentrations of SIM (10 μM and 10 nM) to investigate the effect on osteoblast viability when exposed to SIM for a sustained time period. A higher LDH activity was generally detected in the medium from scaffolds with 10 μM SIM compared to scaffolds with 10 nM SIM throughout the 14-day period. Neither of the SIM concentrations caused a significant increase in LDH activity compared to the effect of alginate-coated scaffolds without SIM. Some variation was seen in the LDH activity profiles, indicating donor-dependent differences in the cellular response to SIM (Figure 4(a)–(c)).

Effect of SIM-containing alginate-coated TiO_2 scaffolds on osteoblast differentiation

Culturing osteoblasts on SIM-containing scaffolds did not significantly change the ALP activity in the culture medium at any of the time points measured either for scaffolds with 10 nM or 10 μM SIM when compared to scaffolds without SIM (Figure 5(a)–(c)). No significant differences were seen in the OPG content of the culture medium at any of the time points either from scaffolds with 10 nM or 10 μM SIM when compared to scaffolds without SIM (Figure 6(a)). However, the content of VEGFA in the culture medium was significantly increased from osteoblasts cultured on scaffolds with both 10 nM and 10 μM SIM when compared to scaffolds without SIM at day 21 ($p = 0.011$, $p = 0.014$) (Figure 6(b)). The secretion of OC was significantly enhanced from osteoblasts on scaffolds with 10 μM SIM when compared to scaffolds without SIM ($p = 0.048$), whereas no significant difference was seen for osteoblasts cultured on scaffolds with 10 nM SIM compared to scaffolds without SIM after 21 days of culture (Figure 6(c)).

After 21 days of culture, the relative expression of *BGLAP* was significantly increased in osteoblasts cultured on scaffolds with 10 μM SIM when compared to scaffolds without SIM and normalized to *GAPDH* ($p = 0.012$). Furthermore, the relative expression of *BMP2* was significantly enhanced in osteoblasts cultured on scaffolds with 10 nM SIM when compared to scaffolds with 10 μM SIM and normalized to *GAPDH* ($p = 0.038$). No significant differences were observed in the expression of *ALPL, COL1A1, TNFRSF11B* or *VEGFA* messenger RNA (mRNA) levels among experimental groups at any of the time points studied (Figure 7).

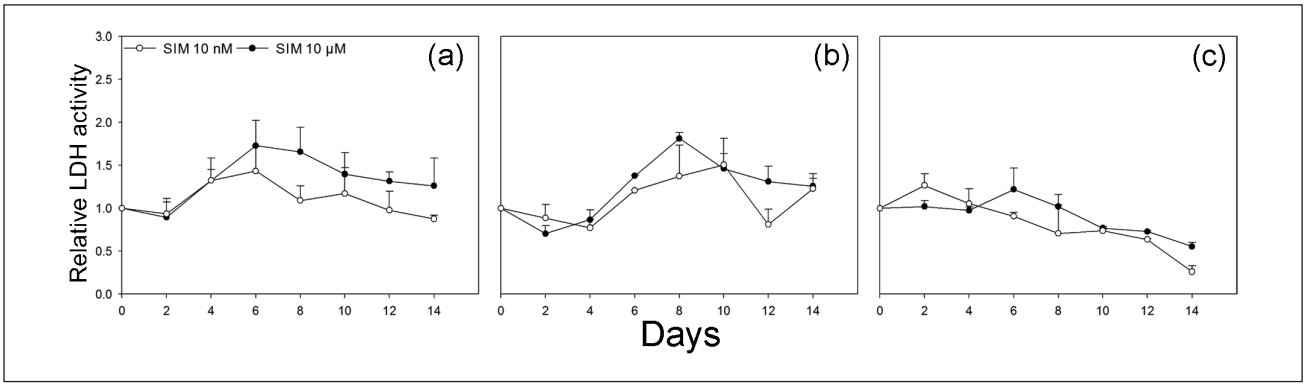

Figure 4. Lactate dehydrogenase (LDH) activity assay. LDH activity in culture medium from scaffolds with 10 nM and 10 µM SIM is shown compared to scaffolds without SIM for (a) donor 1, (b) donor 2 and (c) donor 3 measured every other day up till 14 days. Neither of the SIM concentrations caused a significant increase in LDH activity compared to the effect of alginate-coated scaffolds without SIM. Values represent the mean ± SD.
SIM: simvastatin; SD: standard deviation.

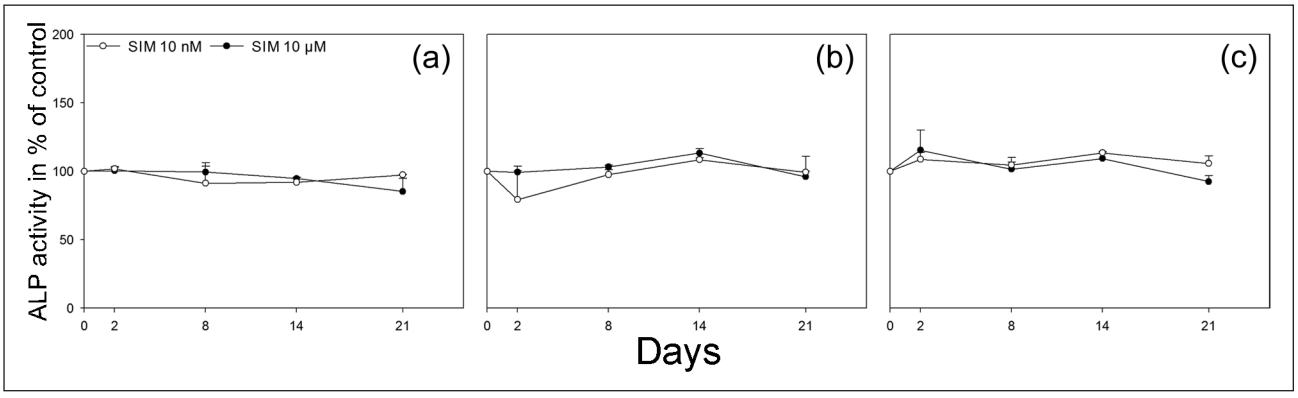

Figure 5. Alkaline phosphatase (ALP) activity assay. ALP activity in culture medium from scaffolds with 10 nM and 10 µM SIM is shown in percentage of control, scaffolds without SIM, for (a) donor 1, (b) donor 2 and (c) donor 3 at 2, 8, 14 and 21 days. ALP activity did not significantly change in the culture medium at any of the time points measured either for scaffolds with 10 nM or 10 µM SIM when compared to scaffolds without SIM. Values represent the mean ± SD.
SIM: simvastatin; SD: standard deviation.

Initiation of matrix mineralization was indicated by significantly elevated calcium content in the culture medium from osteoblasts cultured on scaffolds with 10 µM SIM when compared to scaffolds without SIM at day 21 ($p = 0.028$) (Figure 8).

To evaluate the effect of SIM on the deposition of type I collagen, CLSM visualization was performed on stained scaffolds. Type I collagen was detected intracellular in the majority of cells in all scaffolds. However, extracellular collagen fibrils were almost absent in scaffolds with SIM regardless of the concentration (Figure 9(a) and (b)), while rich networks of type I collagen fibrils were seen in the scaffolds without SIM (Figure 9(c)).

Discussion

The aim was to develop a bone graft material as SIM delivery vehicle for stimulation of bone cell activity. In the present study, we have combined alginate hydrogel with TiO_2 scaffolds to create a SIM delivery system for load-bearing bone tissue applications. SIM is known to enhance osteoblast function in vitro[33,34] and increase bone mass in vivo when injected subcutaneously or administered orally in rodents.[35] Nevertheless, reports regarding the effects of SIM on bone formation in humans are rather inconclusive. While some investigations in osteoporotic patients have described an increase in bone mass and a reduced fracture risk,[36,37] other studies have shown no significant effect of SIM treatment.[38–40] Less than 5% of an oral SIM dose reaches systemic circulation, which in combination with a poor distribution of SIM in the body[41] might result in too low local concentration of SIM in the bone compartment to have an effect on bone metabolism. Local application of SIM might therefore be beneficial to improve the effect on bone metabolism and reduce the toxic side effects caused by high doses of systemically administered SIM.

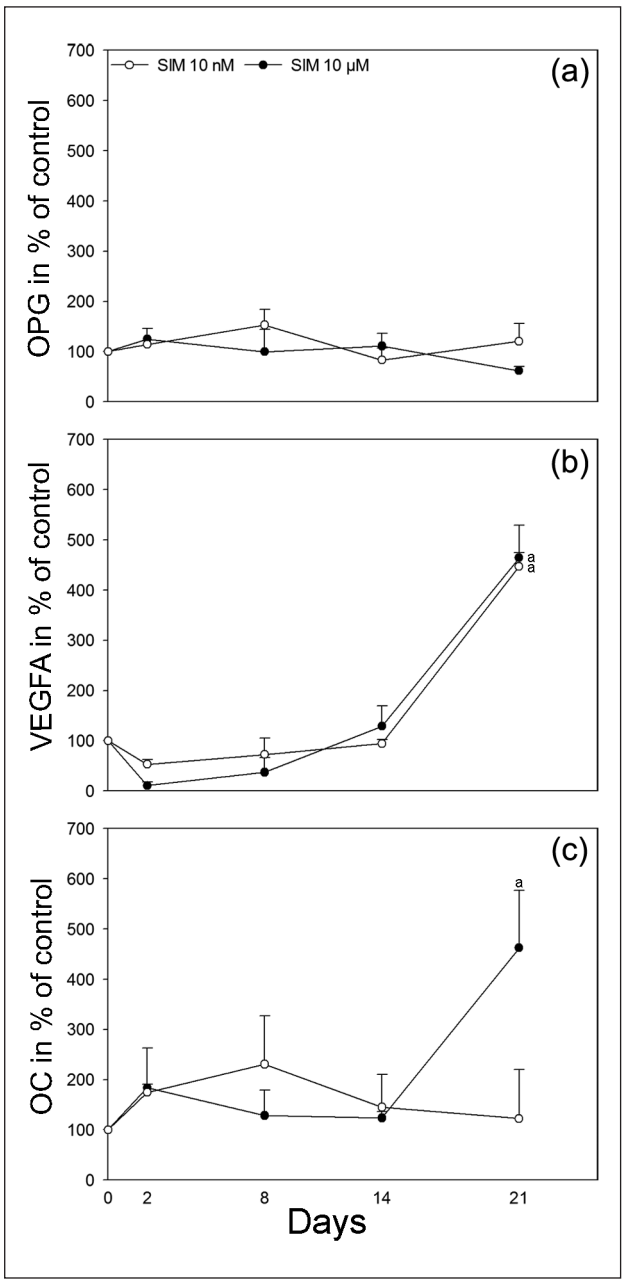

Figure 6. Immunoassay: Quantification of secreted proteins. Secretion of (a) OPG, (b) VEGFA and (c) OC to cell culture medium from scaffolds with 10 nM and 10 µM SIM is shown in percentage of control, scaffolds without SIM, at 2, 8, 14 and 21 days. Values represent the mean ± SD. Statistical analysis: (a) $p \leq 0.05$ versus alginate-coated scaffold without SIM.
SIM: simvastatin; OPG: osteoprotegerin; OC: osteocalcin; VEGFA: vascular endothelial growth factor A; SD: standard deviation.

Alginate hydrogels are widely used for sustained and localized delivery of traditional low-molecular-weight drugs and macromolecules,[42] and it has previously been reported that alginate hydrogels constitute a suitable carrier for SIM delivery at local site.[11] Furthermore, it is often used in composite bone graft materials[43–45] because of its excellent biocompatibility and low immunogenicity.[46] Coating scaffolds with SIM-containing alginate resulted in a progressive and sustained release of SIM, as demonstrated for concentrations of 2.4 and 0.6 mM SIM. Even though TiO_2 scaffolds coated with 24 µM SIM resulted in release of SIM below the limit of detection, it excessively impaired osteoblast viability. Acceptable cell viability was only accomplished with even lower concentrations of SIM (10 µM and below), which is in agreement with previous reports on cell safety and biocompatibility of SIM.[13,33]

The expression of early osteoblast markers (*COL1A1, TNFRSF11B*) in osteoblasts cultured on scaffolds coated with low levels of SIM (10 nM and 10 µM) was not significantly changed. Interestingly, after 21 days of culture, a reduction in type I collagen deposition was in contrast seen in the extracellular matrix of osteoblasts cultured on scaffolds containing SIM. Being a marker of preosteoblasts, a reduction in *COL1A1* is also an indication of osteoblast maturation,[47] implying that osteoblasts cultured on scaffolds with SIM might have grown into a more matured stage compared to the osteoblasts cultured on scaffolds without SIM. Furthermore, COL1A1 synthesis and secretion into the extracellular matrix involve a series of post-translational modifications. For example, a critical step is the hydroxylation of proline residues of collagen chains, a reaction catalysed by prolyl hydroxylases.[48] SIM could decrease the activity of prolyl hydroxylases, as demonstrated previously[49,50] and thereby reduce COL1A1 deposition in the extracellular matrix.

In contrast to the early osteoblast markers, scaffolds with both 10 nM and 10 µM SIM significantly enhanced the secretion of VEGFA from osteoblasts after 21 days of culture. VEGFA is known to regulate osteoblast differentiation[51] as well as increase vascularization during bone formation.[52] Furthermore, it has been shown that compressive loading can considerably stimulate secretion of VEGFA.[53–55] Therefore, in load-bearing bone tissue applications with TiO_2 scaffolds coated with SIM, VEGFA could play even more eminent role in bone gain. Furthermore, SIM significantly enhanced expression of OC on both mRNA and protein levels, confirming that scaffolds with SIM promote osteoblast differentiation. OC is secreted by osteoblasts at the time of bone calcification[56] and is hence a marker of late osteoblast differentiation. Increase in OC levels was however only seen when osteoblasts were cultured on scaffolds with 10 µM SIM and not in scaffolds with 10 nM SIM. In addition, initiation of extracellular matrix mineralization, endpoint for full maturation of the osteoblast phenotype,[57] was shown by elevated calcium secretion from osteoblasts cultured on scaffolds with 10 µM SIM. This dose-dependent regulation of osteoblast differentiation combined with the high cytotoxicity at higher concentrations indicates that a very tight regulation is needed to allow for optimal bone repair if SIM is used locally.

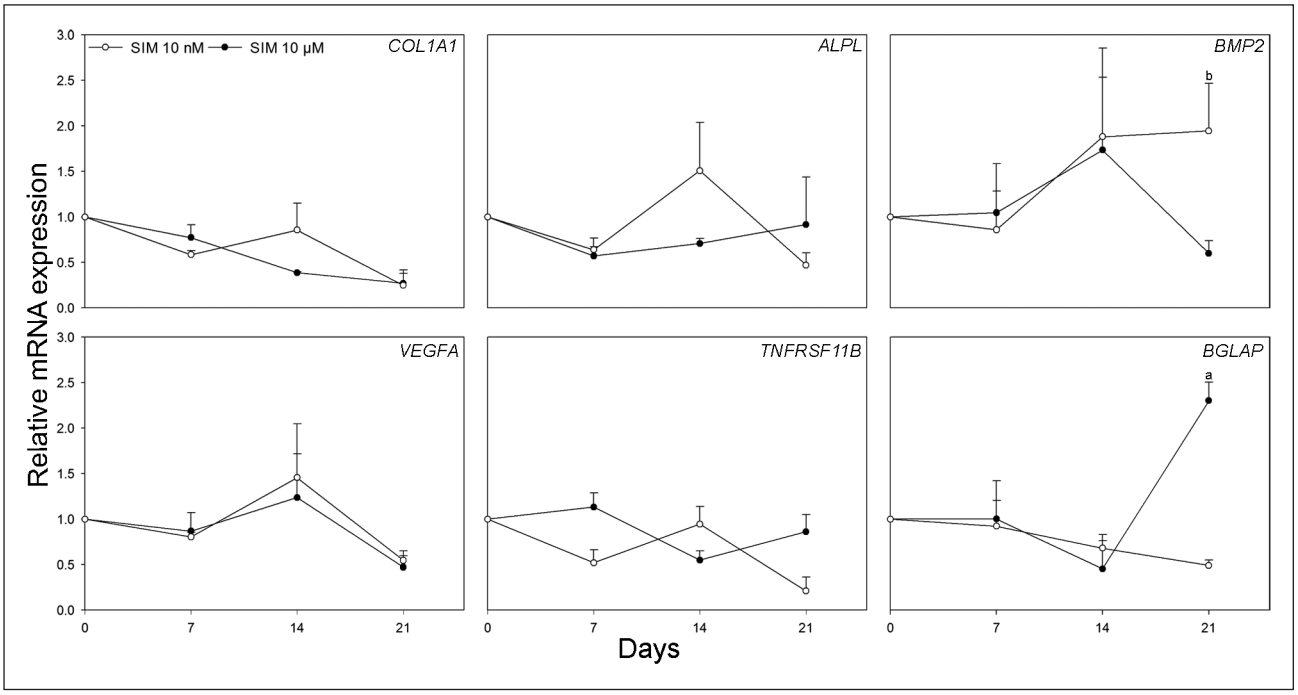

Figure 7. Real-time RT-PCR analysis. Relative mRNA expression levels for *COL1A1, ALPL, BMP2, VEGFA, TNFRSF11B* and *BGLAP* are shown in osteoblasts cultured on scaffolds with 10 nM and 10 µM SIM compared to scaffolds without SIM and normalized to reference gene *GAPDH* at 7, 14 and 21 days. Values represent the mean ± SD. Statistical analysis: (a) $p \leq 0.05$ versus alginate-coated scaffold without SIM and (b) $p \leq 0.05$ versus alginate-coated scaffold with SIM 10 µM.
SIM: simvastatin; RT-PCR: reverse transcriptase–polymerase chain reaction; mRNA: messenger RNA; *GAPDH*: glyceraldehyde-3-phosphate dehydrogenase; *COL1A1:* collagen type I alpha 1; *ALPL:* alkaline phosphatase; *BMP2:* bone morphogenetic protein 2; *VEGFA:* vascular endothelial growth factor A; *TNFRSF11B:* osteoprotegerin; BGLAP: osteocalcin; SD: standard deviation.

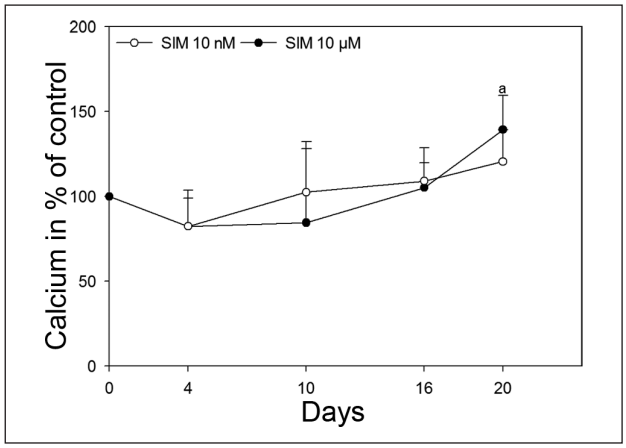

Figure 8. Calcium analysis. Secretion of calcium to cell culture medium from scaffolds with 10 nM and 10 µM SIM is shown in percentage of control, scaffolds without SIM, at 4, 10, 16 and 20 days. Values represent the mean ± SD. Statistical analysis: (a) $p \leq 0.05$ versus alginate-coated scaffold without SIM.
SIM: simvastatin; SD: standard deviation.

The intimate action mechanism of SIM in inducing bone formation is not fully understood. The osteoblast-differentiating effect may be explained by a *BMP2*-mediated action as described previously.[34,35] In the present study, a significant increase in *BMP2* mRNA expression was found in osteoblasts cultured on scaffolds with 10 nM SIM, thus further supporting this mechanism.

As we have shown, SIM could be released from alginate in a slow sustained manner. Nevertheless, in bone tissue engineering, the structure of the scaffold should provide load-bearing capabilities and an optimal microenvironment for osteogenesis.[24,30] The scaffold porosity, pore network interconnectivity, surface-area-to-volume ratio and the physico-chemical properties of the surface determine the cell migration and differentiation, bone ingrowth, vascularization and mass transfer between the cells and the environment.[22] It has previously been demonstrated that TiO_2 scaffolds can provide an appropriate surface for osteoblasts to adhere, migrate, proliferate and differentiate.[25–28] In this study, as revealed by SEM and micro-CT, TiO_2 scaffolds were successfully coated with alginate hydrogel to gain benefit of alginate drug release capabilities. Alginate infiltrated into the scaffold covering the strut surfaces uniformly, while leaving the 3D structure and physical properties of the TiO_2 scaffold intact. Therefore, production of bone graft material as vehicle for SIM delivery was feasible without compromising the desired pore architectural characteristics of the TiO_2 scaffold.

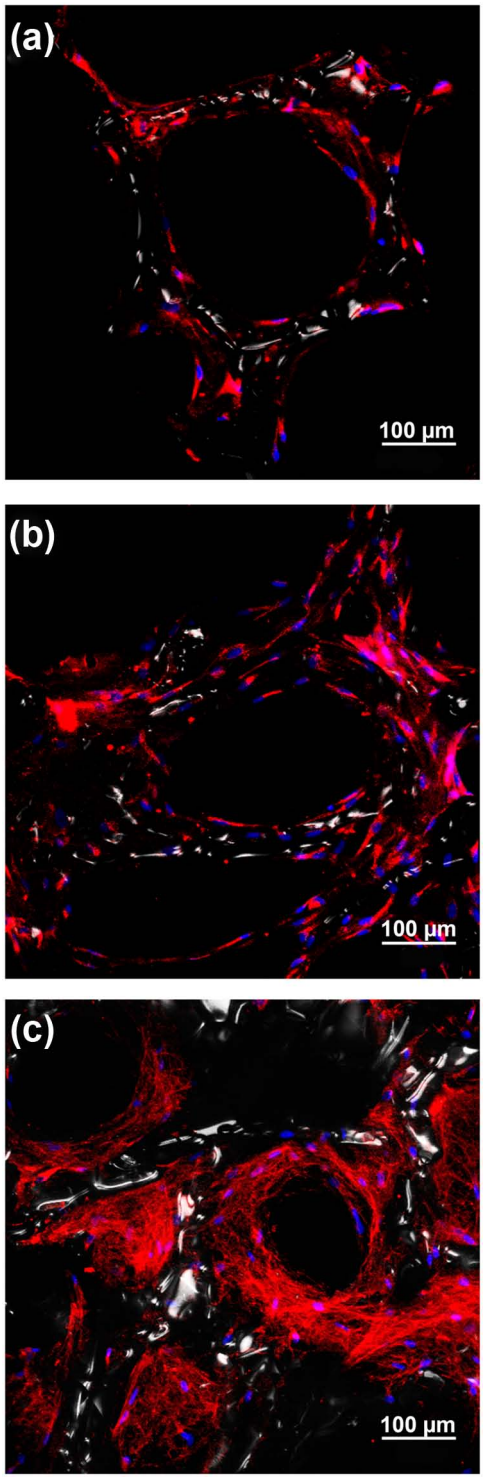

Figure 9. Confocal laser scanning microscopy visualization of type I collagen deposition in alginate-coated TiO_2 scaffolds with or without simvastatin (SIM). Fluorescence immunocytochemical analysis of type I collagen in primary human osteoblasts cultured on alginate-coated TiO_2 scaffolds. Type I collagen is detected in the majority of the cells cultured on scaffolds with (a) 10 nM SIM, (b) 10 µM SIM and (c) without SIM. Extracellular collagen fibrils are only seen in scaffold (c) without SIM. Type I collagen (red), DNA (blue), TiO_2 scaffold surface (white).

Conclusion

In conclusion, the study shows that alginate-coated TiO_2 scaffolds can act as a matrix for SIM delivery inducing osteoblast cell differentiation. Scaffolds coated with alginate hydrogel containing 10 µm SIM had low cytotoxicity and significantly increased the secretion of VEGFA and OC from osteoblasts cultured on the scaffolds. The combination of the local osteogenic effect of SIM and the physical properties of the TiO_2 scaffolds may represent a new strategy for bone tissue regeneration in load-bearing bone.

Acknowledgements

The authors acknowledge Aina Mari Lian, Grazyna Jonski and Jonas Wengenroth for their help and expertise with immunoassay, atomic absorption spectroscopy and micro-computed tomography, respectively (Faculty of Dentistry, Oral Research Laboratory, University of Oslo, Oslo, Norway).

Declaration of conflicting interests

The authors declare that there is no conflict of interest.

Funding

This study was supported by the Norwegian Research Council grants 228415 and 201596. The open-access fee was generously provided by the University of Oslo's Publication fund.

References

1. Giannoudis PV, Chris Arts JJ, Schmidmaier G, et al. What should be the characteristics of the ideal bone graft substitute? *Injury* 2011; 42(Suppl. 2): S1–S2.
2. Dimitriou R, Mataliotakis GI, Angoules AG, et al. Complications following autologous bone graft harvesting from the iliac crest and using the RIA: a systematic review. *Injury* 2011; 42(Suppl. 2): S3–S15.
3. Ben-David D, Srouji S, Shapira-Schweitzer K, et al. Low dose BMP-2 treatment for bone repair using a PEGylated fibrinogen hydrogel matrix. *Biomaterials* 2013; 34(12): 2902–2910.
4. Zieris A, Chwalek K, Prokoph S, et al. Dual independent delivery of pro-angiogenic growth factors from star-PEG-heparin hydrogels. *J Control Release* 2011; 156(1): 28–36.
5. Zheng F, Wang S, Wen S, et al. Characterization and antibacterial activity of amoxicillin-loaded electrospun nano-hydroxyapatite/poly(lactic-*co*-glycolic acid) composite nanofibers. *Biomaterials* 2013; 34(4): 1402–1412.
6. Monjo M, Rubert M, Ellingsen J, et al. Rosuvastatin promotes osteoblast differentiation and regulates SLCO1A1 transporter gene expression in MC3T3-E1 cells. *Cell Physiol Biochem* 2010; 26(4–5): 647–656.
7. Vo TN, Kasper FK and Mikos AG. Strategies for controlled delivery of growth factors and cells for bone regeneration. *Adv Drug Deliver Rev* 2012; 64(12): 1292–1309.
8. Park YS, David AE, Park KM, et al. Controlled release of simvastatin from in situ forming hydrogel triggers bone formation in MC3T3-E1 cells. *AAPS J* 2013; 15(2): 367–376.

9. Bae MS, Yang DH, Lee JB, et al. Photo-cured hyaluronic acid-based hydrogels containing simvastatin as a bone tissue regeneration scaffold. *Biomaterials* 2011; 32(32): 8161–8171.
10. Wadagaki R, Mizuno D, Yamawaki-Ogata A, et al. Osteogenic induction of bone marrow-derived stromal cells on simvastatin-releasing, biodegradable, nano- to microscale fiber scaffolds. *Ann Biomed Eng* 2011; 39(7): 1872–1881.
11. Ito T, Saito M, Uchino T, et al. Preparation of injectable auto-forming alginate gel containing simvastatin with amorphous calcium phosphate as a controlled release medium and their therapeutic effect in osteoporosis model rat. *J Mater Sci: Mater M* 2012; 23(5): 1291–1297.
12. Liao JK and Laufs U. Pleiotropic effects of statins. *Annu Rev Pharmacol* 2005; 45: 89–118.
13. Pagkalos J, Cha JM, Kang Y, et al. Simvastatin induces osteogenic differentiation of murine embryonic stem cells. *J Bone Miner Res* 2010; 25(11): 2470–2478.
14. Ahn KS, Sethi G, Chaturvedi MM, et al. Simvastatin, 3-hydroxy-3-methylglutaryl coenzyme A reductase inhibitor, suppresses osteoclastogenesis induced by receptor activator of nuclear factor-kappaB ligand through modulation of NF-kappaB pathway. *Int J Cancer* 2008; 123(8): 1733–1740.
15. Fukui T, Ii M, Shoji T, et al. Therapeutic effect of local administration of low-dose simvastatin-conjugated gelatin hydrogel for fracture healing. *J Bone Miner Res* 2012; 27(5): 1118–1131.
16. Monjo M, Rubert M, Wohlfahrt JC, et al. In vivo performance of absorbable collagen sponges with rosuvastatin in critical-size cortical bone defects. *Acta Biomater* 2010; 6(4): 1405–1412.
17. Walter MS, Frank MJ, Rubert M, et al. Simvastatin-activated implant surface promotes osteoblast differentiation in vitro. *J Biomater Appl*. Epub ahead of print 2 May 2013. DOI: 10.1177/0885328213486364.
18. Nyan M, Hao J, Miyahara T, et al. Accelerated and enhanced bone formation on novel simvastatin-loaded porous titanium oxide surfaces. *Clin Implant Dent R*. Epub ahead of print 7 February 2013. DOI: 10.1111/cid.12045.
19. Chu TM, Warden SJ, Turner CH, et al. Segmental bone regeneration using a load-bearing biodegradable carrier of bone morphogenetic protein-2. *Biomaterials* 2007; 28(3): 459–467.
20. Kolambkar YM, Dupont KM, Boerckel JD, et al. An alginate-based hybrid system for growth factor delivery in the functional repair of large bone defects. *Biomaterials* 2011; 32(1): 65–74.
21. Nath SD, Linh NT, Sadiasa A, et al. Encapsulation of simvastatin in PLGA microspheres loaded into hydrogel loaded BCP porous spongy scaffold as a controlled drug delivery system for bonetissue regeneration. *J Biomater Appl*. Epub ahead of print 12 September 2013. DOI: 10.1177/0885328213499272.
22. Hutmacher DW. Scaffolds in tissue engineering bone and cartilage. *Biomaterials* 2000; 21(24): 2529–2543.
23. Bose S, Roy M and Bandyopadhyay A. Recent advances in bone tissue engineering scaffolds. *Trends Biotechnol* 2012; 30(10): 546–554.
24. Tiainen H, Wiedmer D and Haugen HJ. Processing of highly porous TiO_2 bone scaffolds with improved compressive strength. *J Eur Ceram Soc* 2013; 33(1): 15–24.
25. Verket A, Tiainen H, Haugen H, et al. Enhanced osteoblast differentiation on scaffolds coated with TiO2 compared to SiO2 and CaP coatings. *Biointerphases* 2012; 7(1–4): 1–10.
26. Sabetrasekh R, Tiainen H, Reseland J, et al. Impact of trace elements on biocompatibility of titanium scaffolds. *Biomed Mater* 2010; 5(1): 015003.
27. Gomez-Florit M, Rubert M, Ramis JM, et al. TiO_2 scaffolds sustain differentiation of MC3T3-E1 cells. *J Biomater Tiss Eng* 2012; 2(4): 336–344.
28. Tiainen H, Wohlfahrt JC, Verket A, et al. Bone formation in TiO_2 bone scaffolds in extraction sockets of minipigs. *Acta Biomater* 2012; 8(6): 2384–2391.
29. Haugen HJ, Monjo M, Rubert M, et al. Porous ceramic titanium dioxide scaffolds promote bone formation in rabbit peri-implant cortical defect model. *Acta Biomater* 2013; 9(2): 5390–5399.
30. Tiainen H, Lyngstadaas SP, Ellingsen J, et al. Ultra-porous titanium oxide scaffold with high compressive strength. *J Mater Sci: Mater M* 2010; 21(10): 2783–2792.
31. Takahashi Y and Tabata Y. Homogeneous seeding of mesenchymal stem cells into nonwoven fabric for tissue engineering. *Tissue Eng* 2003; 9(5): 931–938.
32. Pfaffl MW. A new mathematical model for relative quantification in real-time RT–PCR. *Nucleic Acids Res* 2001; 29(9): e45.
33. Ruiz-Gaspa S, Nogues X, Enjuanes A, et al. Simvastatin and atorvastatin enhance gene expression of collagen type 1 and osteocalcin in primary human osteoblasts and MG-63 cultures. *J Cell Biochem* 2007; 101(6): 1430–1438.
34. Maeda T, Matsunuma A, Kurahashi I, et al. Induction of osteoblast differentiation indices by statins in MC3T3-E1 cells. *J Cell Biochem* 2004; 92(3): 458–471.
35. Mundy G, Garrett R, Harris S, et al. Stimulation of bone formation in vitro and in rodents by statins. *Science* 1999; 286(5446): 1946–1949.
36. Chan KA, Andrade SE, Boles M, et al. Inhibitors of hydroxymethylglutaryl-coenzyme A reductase and risk of fracture among older women. *Lancet* 2000; 355(9222): 2185–2188.
37. Solomon DH, Finkelstein JS, Wang PS, et al. Statin lipid-lowering drugs and bone mineral density. *Pharmacoepidem Dr S* 2005; 14(4): 219–226.
38. Rejnmark L, Buus HN, Vestergaard P, et al. Effects of simvastatin on bone turnover and BMD: a 1-year randomized controlled trial in postmenopausal osteopenic women. *J Bone Miner Res* 2004; 19(5): 737–744.
39. Wada Y, Nakamura Y and Koshiyama H. Lack of positive correlation between statin use and bone mineral density in Japanese subjects with type 2 diabetes. *Arch Intern Med* 2000; 160(18): 2865.
40. Van Staa T-P, Wegman S, De Vries F, et al. Use of statins and risk of fractures. *JAMA* 2001; 285(14): 1850–1855.
41. Bellosta S, Bernini F, Paoletti R, et al. Non-lipid-related effects of statins. *Ann Med* 2000; 32(3): 164–176.
42. Langer R. Drug delivery and targeting. *Nature* 1998; 392: (Suppl. 6679): 5–10.
43. Zhang SM, Cui FZ, Liao SS, et al. Synthesis and biocompatibility of porous nano-hydroxyapatite/collagen/alginate composite. *J Mater Sci: Mater M* 2003; 14(7): 641–645.
44. Luginbuehl V, Wenk E, Koch A, et al. Insulin-like growth factor I-releasing alginate-tricalciumphosphate composites for bone regeneration. *Pharm Res* 2005; 22(6): 940–950.

45. Lin HR and Yeh YJ. Porous alginate/hydroxyapatite composite scaffolds for bone tissue engineering: preparation, characterization, and in vitro studies. *J Biomed Mater Res B* 2004; 71(1): 52–65.
46. Shapiro L and Cohen S. Novel alginate sponges for cell culture and transplantation. *Biomaterials* 1997; 18(8): 583–590.
47. Stein GS, Lian JB, Stein JL, et al. Transcriptional control of osteoblast growth and differentiation. *Physiol Rev* 1996; 76(2): 593–629.
48. Prockop DJ and Kivirikko KI. Heritable diseases of collagen. *N Engl J Med* 1984; 311(6): 376–386.
49. Thirunavukkarasu M, Selvaraju V, Dunna NR, et al. Simvastatin treatment inhibits hypoxia inducible factor 1-alpha-(HIF-1alpha)-prolyl-4-hydroxylase 3 (PHD-3) and increases angiogenesis after myocardial infarction in streptozotocin-induced diabetic rat. *Int J Cardiol* 2013; 168(3): 2474–2480.
50. Ahmad T, Kumar M, Mabalirajan U, et al. Hypoxia response in asthma. *Am J Resp Cell Mol* 2012; 47(1): 1–10.
51. Mayr-Wohlfart U, Waltenberger J, Hausser H, et al. Vascular endothelial growth factor stimulates chemotactic migration of primary human osteoblasts. *Bone* 2002; 30(3): 472–477.
52. Schmid J, Wallkamm B, Hämmerle CH, et al. The significance of angiogenesis in guided bone regeneration. A case report of a rabbit experiment. *Clin Oral Implan Res* 2002; 8(3): 244–248.
53. Faure C, Linossier M-T, Malaval L, et al. Mechanical signals modulated vascular endothelial growth factor-A (VEGF-A) alternative splicing in osteoblastic cells through actin polymerisation. *Bone* 2008; 42(6): 1092–1101.
54. Dumas V, Perrier A, Malaval L, et al. The effect of dual frequency cyclic compression on matrix deposition by osteoblast-like cells grown in 3D scaffolds and on modulation of VEGF variant expression. *Biomaterials* 2009; 30(19): 3279–3288.
55. Faure C, Vico L, Tracqui P, et al. Functionalization of matrices by cyclically stretched osteoblasts through matrix targeting of VEGF. *Biomaterials* 2010; 31(25): 6477–6484.
56. Vermeulen A, Vermeer C and Bosman FT. Histochemical detection of osteocalcin in normal and pathological human bone. *J Histochem Cytochem* 1989; 37(10): 1503–1508.
57. Lian JB and Stein GS. Concepts of osteoblast growth and differentiation: basis for modulation of bone cell development and tissue formation. *Crit Rev Oral Biol M* 1992; 3(3): 269–305.